

Photochemistry and Photophysics of (*p*-Benzoylphenyl)diphenylmethyl and (*p*-Benzoylphenyl)bis(4-*tert*-butylphenyl)methyl Radicals in Different Solvents

Viktor V. Jarikov, Alexandre V. Nikolaitchik, and Douglas C. Neckers*

Center for Photochemical Sciences, Bowling Green State University, Bowling Green, Ohio 43403

Received: January 18, 2000; In Final Form: March 23, 2000

The photochemical reactions of (*p*-benzoylphenyl)diphenylmethyl (**1**) and (*p*-benzoylphenyl)bis(4-*tert*-butylphenyl)methyl (**2**) in various solvents were investigated. The photophysical parameters of the first excited doublet state of the radicals were measured using spectroscopic and kinetic methods and led to a “molecular rotor” model to characterize the excited-state behavior. The charge-transfer excited state for both radicals was observed. Photoproducts separated from the photolysis of **1** and **2** in benzene suggest photodecomposition proceeds via H-abstraction (55%), fragmentation (20%), cyclization (10%), and addition (10%).

Introduction

Resonance stabilization and steric hindrance are major factors in determining the stability of a free radical. Since 1900, when Gomberg first prepared a stable compound with trivalent carbon,² numerous triarylmethyl (TAM), aryloxy, and nitroxyl stable free radicals have been discovered and characterized.³ The photochemistry and photophysics of arylmethyl radicals has been reviewed.^{4–10}

The intramolecular chemistry of excited radicals has been shown to involve cleavage, photoionization, and cyclization reactions, which are normally not observed for ground-state radicals.⁴ The intramolecular photochemistry of triphenylmethyl (TPM) was first investigated by Letsinger et al.¹¹ and recently revisited in detail by Siskos et al.¹² 9-Phenylfluorene-derived photoproducts were identified from the photolysis of this and similar radicals.¹³ On the other hand, excitation of tri- and diarylmethyl radicals in polar solvents results in formation of the corresponding cations and ϵ_{solv} , as reported by several workers.^{12,14} Although suggested on the basis of the photoproduct studies,¹⁵ carbene formation via excited-radical chemistry in solution at room temperature remains to be proved, for example, by the way of trapping.⁴

The intermolecular photochemistry of radicals has been shown to include enhanced electron-donor and -acceptor properties, H-abstraction, and physical quenching by oxygen.^{4,5} Photoinduced electron-transfer reactions of the first excited doublet states of TAM radicals with amines ($k \sim 10^8\text{--}10^{10} \text{ M}^{-1} \text{ s}^{-1}$),¹³ halogenated hydrocarbons and arenes ($\phi_{\text{cation}} \sim 100\%$),⁴ and methyl viologen¹⁶ have been reported.

Recently, a number of reports on the chemistry of TAM radicals have been published.^{17–20} Renewed research efforts in the area are directed at the investigation of the resonance stabilization and “captodative” stabilization of stable radicals.^{17,18} ESR and ENDOR are the major methods used for the investigations. The hyperfine coupling constants of TAM radicals depend on the overall conformation of the molecule. A twist angle of about 32° for the benzene rings in the TPM radical was determined by Adrian.²¹ Since no significant change in hyperfine coupling constant as well as in width of the ESR signal occurs upon para-substitution, the conformation of the para-substituted TPM radicals is the same as that of the TPM radical.

In the present work we focus on the photophysical properties and photochemical reactions of (*p*-benzoylphenyl)diphenylmethyl (**1**)²² and its di-*tert*-butylated derivative, (*p*-benzoylphenyl)bis(4-*tert*-butylphenyl)methyl (**2**).^{15,23,24} The resonance structures of **1** and **2** can be divided into three major groups. In the first the unpaired electron is located on the carbon atoms of the radical; in the second it is localized on the oxygen atom; and the third contains charge-transfer (Scheme 1) type structures. The “*g*-values” of **1** (2.0029),¹⁸ **2**, and other substituted TPM radicals (2.0026–2.0035)^{17,18} indicate that they are carbon-centered radicals; hence the first group of resonance structures may dominate. The photochemistry of **1** in solution is complicated due to significant formation of the dimer. However, **2** should be fully dissociated in solution because all the reactive para-positions are hindered by bulky substituents.²³

Results and Discussion

I. (*p*-Benzoylphenyl)diphenylmethyl (1**). (a) Characterization.** Radical **1** was synthesized from chloride **4** using Ag powder in a number of solvents such as hexane, benzene, acetone, acetonitrile, and adiponitrile. Solvent polarity has a minor effect on the absorption spectrum of **1** ($\lambda_{\text{max}} = 582\text{--}584$ nm in acetonitrile or benzene, Figures 1A and 2A), indicating that insignificant change in the radical dipole moment is associated with the absorption process. On the other hand, a red shift and change of the spectral shape of the fluorescence of **1** occurs in polar solvents (Figure 1B). This points to a significant dipole moment of the excited D₁ state as well as possible existence of a state with different energy.

In fluid solution **1** undergoes reversible exothermic dimerization. The structure of dimer **5** was determined by NMR spectroscopy (Scheme 2).¹⁸ Compound **6**, obtained via an acid-catalyzed H[1,5] shift in **5**, serves as additional evidence for the structure of **5**.²⁵ The thermodynamics of dimerization was studied by Neumann et al. using an ESR technique.^{17,18} By dissolving a known amount of the dimer in toluene, measuring the intensity of the ESR signal, and comparing it to a standard signal from diphenylpicrylhydrazyl, a degree of dissociation of the dimer (α) at a given temperature could be calculated. A value of 33% was obtained for a 0.01 M solution of **5** in benzene

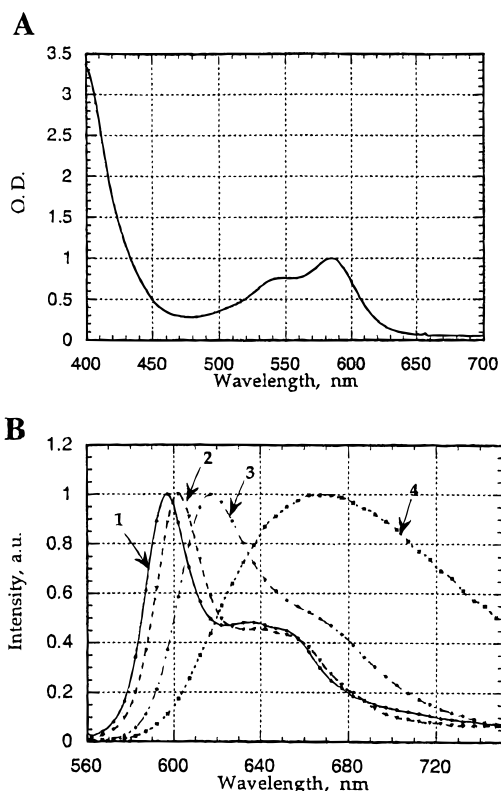
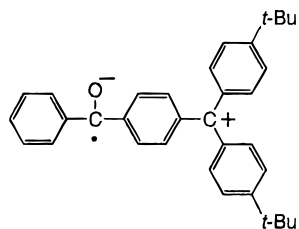
SCHEME 1: Structure Corresponding to the CT State of 2

Figure 1. (A) Absorption spectrum of **1** in benzene ($[4] = 1.12 \times 10^{-3}$ M). (B) Normalized fluorescence spectra of **1** ($\lambda_{\text{exc}} = 540$ nm): (1) hexane, (2) mineral oil, (3) benzene, (4) acetonitrile.

at 25 °C. A value of 10.3 ± 0.1 kcal/mol was obtained for the ΔH of dissociation of **5** based on the study of the temperature effect.

The equilibrium concentrations of **1** and **5** can be calculated on the basis of the dimerization equilibrium constant,^{18,26} $K = 308 \text{ M}^{-1}$, and $[1]_0$ ($[1]_0 = [4]$) assuming quantitative conversion of the starting chloride **4**; negative Beilstein²⁷ test). Thus, one can plot $[1]_{\text{eq}}/[5]_{\text{eq}}$ as a function $[1]_0$ in benzene (Figure 3).²³ This plot indicates that the dimer is the dominating species in benzene when $[1]_0 > 3 \times 10^{-3}$ M.

The presence of dimer **5** can be observed indirectly by measuring the fluorescence of **1** in solution. The absorption and fluorescence spectra of **1** in acetonitrile are shown in Figure 2. The fluorescence spectra of **1** were measured with 400 nm excitation where all the light was absorbed. As $[1]_0$ increased from sample #1 to sample #4, the fluorescence intensity decreased. This is explained by the presence of quinoid dimer **5**, which absorbs at 400 nm as well. As $[1]_0$ increases, so does $[5]_{\text{eq}}$. At higher $[1]_0$, the ratio $[1]_{\text{eq}}/[5]_{\text{eq}}$ is smaller than at lower $[1]_0$ (Figure 3); hence $[21^*]$ and subsequently fluorescence intensity decrease. Lower fluorescence intensity at higher $[1]_0$ can also be explained by self-quenching of **1**, which may produce even more of **5** via the Pschorr reaction.^{28,29}

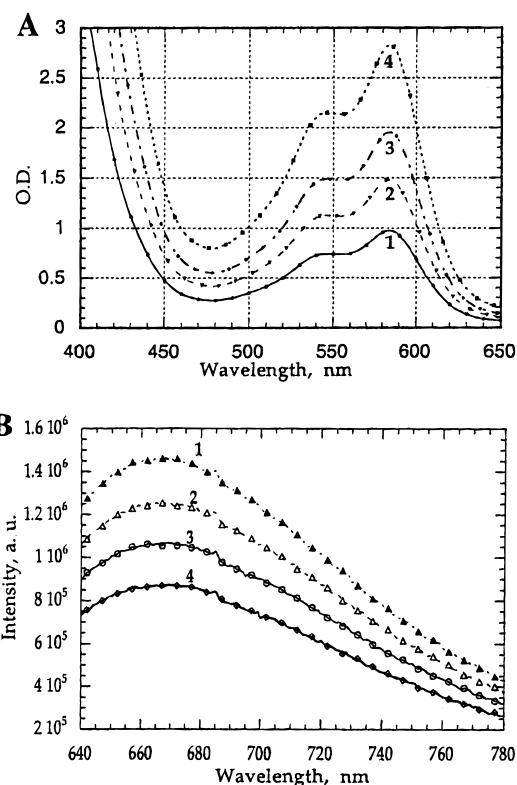


Figure 2. Absorption (A) and fluorescence (B, $\lambda_{\text{exc}} = 400$ nm) spectra of **1** in acetonitrile, $[1]_0$: (1) 1.125×10^{-3} M, (2) 2.745×10^{-3} M, (3) 4.191×10^{-3} M, (4) 6.764×10^{-3} M.

Assuming that Beer's law is valid in the 10^{-4} – 10^{-3} M range, the dimerization equilibrium constant in acetonitrile, $K = 20\,300 \text{ M}^{-1}$ and the extinction coefficient at 584 nm, $\epsilon = 6300$ could be calculated from the absorption spectra in Figure 2. This indicates that the equilibrium shifts toward the dimer in more polar solvents.

Both the ground-state D_0 and the first excited-state D_1 of **1** have doublet multiplicity. To determine whether the quartet state of **1** is populated by intersystem crossing from D_1 , emission from excited **1** in rigid organic glass was studied. Dimerization of **1** is an exothermic process, thus the lower the temperature the greater $[5]$ and the lower $[1]$. Therefore, a cooling step was carried out as quickly as possible. Two methods were used to study **1** in the methyltetrahydrofuran (MeTHF) glass at 77 K. In method #1 **1** was produced by addition of Ag to the solution of chloride **4** in degassed MeTHF at 25 °C. This was followed by rapid cooling in liquid nitrogen, and a fraction of **1** was trapped in the solid. In method #2, chloride precursor **4** was dissolved in degassed MeTHF at 25 °C, the solution was cooled in liquid nitrogen and irradiated with 366 nm light. The irradiation of the chloride led to homolysis and formation of **1**. Both samples were examined for emission in the 600–800 nm range with different delay times ($\lambda_{\text{exc}} = 580$ nm). Absence of the observed emission signal suggests that the quartet state of **1** is not populated.

The two samples differed depending on the method of preparation. Radical **1** synthesized at 25 °C in solution was red (#1), while that prepared in MeTHF glass at 77 K via irradiation was blue (#2). The fluorescence excitation and emission spectra of the two samples are shown in Figure 4. The red 15 nm shift in the fluorescence excitation spectrum of **1** in sample #2 explains the difference in color between the samples. This difference could come from the presence of the chlorine atom in the matrix of sample #2. However, when the same experi-

SCHEME 2: Dimerization of 1

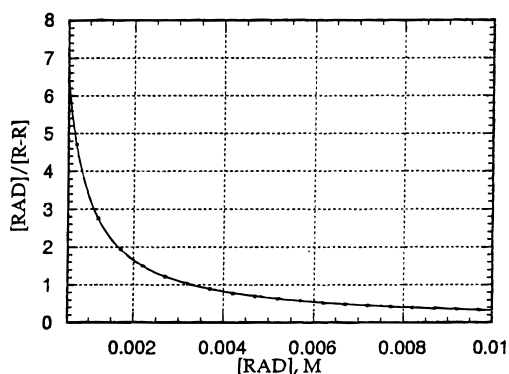
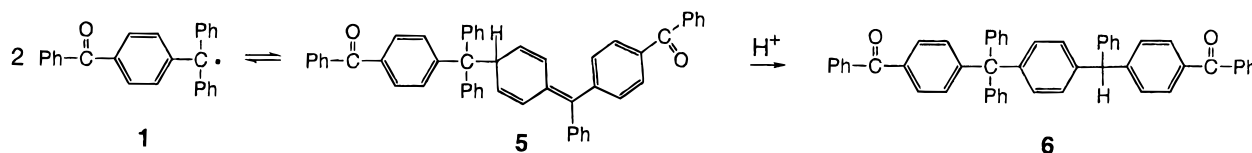


Figure 3. Ratio $[1]_{\text{eq}}/[5]_{\text{eq}}$ as a function of $[1]_0$ in benzene at 25 °C.

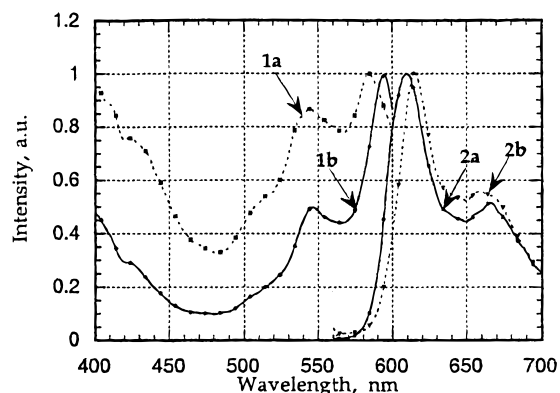


Figure 4. Fluorescence excitation (1a, 1b) and emission (2a, 2b) spectra of **1** in MeTHF glass at 77 K: (1a, 2a) synthesized in solution (#1); (1b, 2b) synthesized in glass (#2).

ments were performed with the TPM radical, no difference was detected between the samples. We propose that the spectral shift is brought about by the difference in the conformation of **1**. In the case of sample #2, the chloride precursor **4** was trapped in a matrix and its conformation was transferred into **1** formed after irradiation, while **1** was trapped in its normal conformation in solution in sample #1.

(b) Photochemistry of 1 in Solution. The photochemistry of **1** in benzene was initially studied by Neckers et al.¹⁵ The products of photolysis with both visible and UV light were found to be essentially the same. They were identified as (*p*-benzoylphenyl)diphenylmethane (**7**) (major), benzophenone (**8**), tetraphenylethylene (**9**), and 1,4-dibenzoylbenzene (**10**) (Scheme 3). When photolysis was performed in benzene-*d*₆ or CD₃CN, no deuterium was incorporated into **7** and **8**. This points to the bimolecular H-abstraction reaction between **1** and **5** or the photolysis products. Quinoid dimer **5** seems one of the most likely H-donors. It appears that products **8**–**10** are formed as a result of a photodissociation of **1**. Ethylene **9** can be formed via coupling reaction of diphenylcarbene, while **10** can come from a recombination reaction of benzophenone radical and benzoyl radical. The efficiency of the reaction is low upon irradiation with both UV and visible light. The quantum yield of the reaction was not measured because of the presence of the dimer, which most probably interfered with the reaction.

When deuterated methanol was added to the solution of **1** in acetonitrile, a spontaneous dark reaction led to formation of (*p*-benzoylphenyl)diphenylmethyl methyl ether (**12**) (major) and (*p*-benzoylphenyl)diphenyldeuteriomethane (**11**) (minor) (Scheme 3). However, a solution of **1** in benzene in the presence of 1 M MeOD was stable in the dark. When the latter was irradiated, **11** and **12** were found in a 1:1 ratio. Deuteriomethane **11** and (*p*-benzoylphenyl)diphenylmethanol (**13**) in a 1:1 ratio were the products of the reaction in acetonitrile in the presence of 1 M D₂O. This reaction was slow in the dark but fast upon irradiation with visible light. The GC/MS analysis of methane **11** (deuterated **7**) formed in the presence of MeOD and D₂O revealed a significant degree of deuteration. We conclude that addition to excited **1** took place indicating significant polarity of **1***

The investigation of **1** is complicated by the **1**–**5** equilibrium, which is affected by solvent. Processes such as fluorescence and photochemical transformations depend on **[5]**, thus numerous corrections are required to obtain concentration-independent values for ϕ_{fl} and the rate constants of the transient decay. Therefore, we determined it preferably to eliminate the quinoid dimer. Dissociation of the dimer is an endothermic process with $\Delta H = 10.3$ kcal/mol at 25 °C in benzene. Therefore, at 70 °C and 10^{-5} M concentration of **1**, **[5]** is reduced to a negligible level. The disadvantage of this approach is the thermal instability of the radical in polar solvents such as acetonitrile.

Magnetic susceptibility and absorption measurements indicate that tris(4-*tert*-butylphenyl)methyl is 100% dissociated in solution at room temperature.³⁰ Therefore, (*p*-benzoylphenyl)bis(4-*tert*-butylphenyl)methyl (**2**) is likely to be 100% dissociated in solution because all three para-positions are blocked with bulky substituents.

II. (*p*-Benzoylphenyl)bis(4-*tert*-butylphenyl)methyl (2**). (a) Characterization.** A relatively small blue shift (4 nm) is observed in the absorption spectra of **2** as the solvent is changed from benzene to acetonitrile (Figure 5A). On the other hand, a significant change in the shape of the fluorescence spectrum of **2** (Figure 5B), as well as in the efficiency of fluorescence, was observed with the increase in solvent polarity. In benzene, the fluorescence spectrum of **2** is a mirror image of the absorption spectrum. Therefore, the first excited doublet state D₁ of **2** may have a rigid structure similar in geometry to that of the ground-state D₀. In benzonitrile and acetonitrile the shape of the spectra differs significantly from that in benzene. A broad emission is observed along with a 50–70 nm red shift in the maximum. Such a large red shift of fluorescence corresponds to an excited state with a significant degree of charge transfer. Quantum yields of fluorescence of **2** vary from 0.44 in benzene to 0.024 in benzonitrile and 1×10^{-3} in acetonitrile. The fluorescence excitation spectrum of **2** in acetonitrile (observation at 712 nm) was identical with the absorption spectrum of **2**, which indicates that the same excited D₁ state is formed initially in acetonitrile.

On the basis of these data the existence of a charge-transfer (CT) state for **2** can be proposed (Scheme 1). In polar solvents this CT state is lower in energy than the D₁ state, thus a rapid transition between the two states takes place. Observation of low ϕ_{fl} and broad structureless emission in polar solvents is

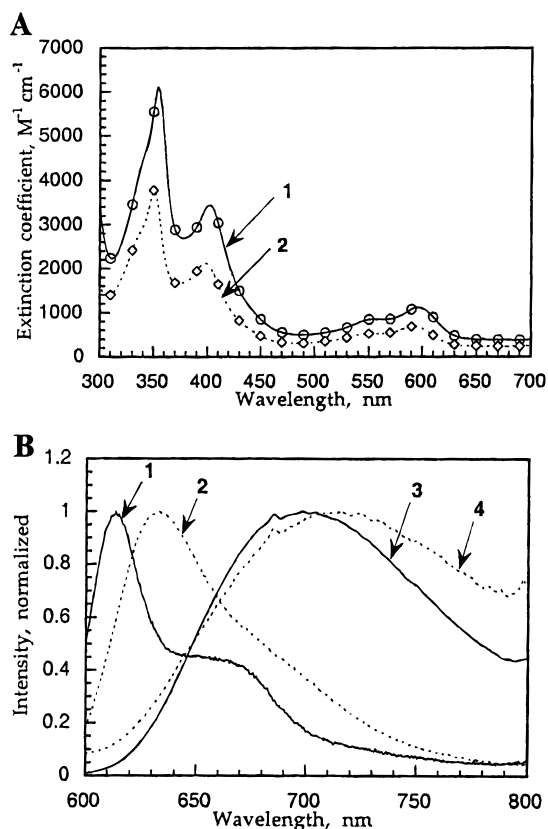
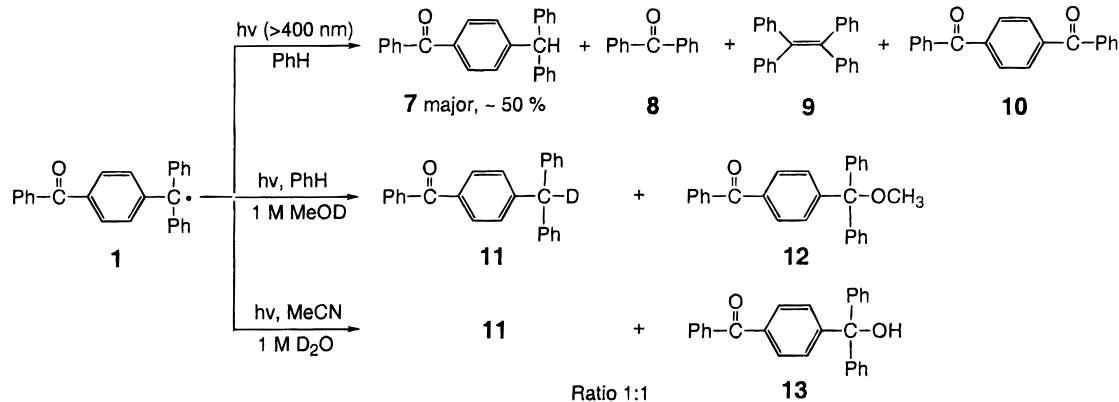
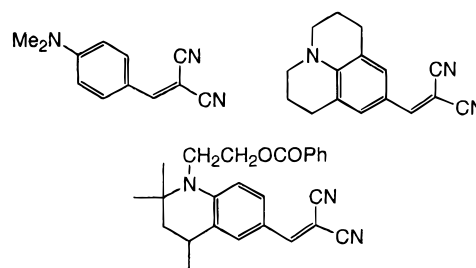
SCHEME 3: Photolysis of 1 (A) in Benzene with Visible Light, (B) in the Presence of MeOD, and (C) in Acetonitrile in the Presence of D₂O

Figure 5. (A) Absorption spectra of **2** in (1) benzene ($\lambda/\epsilon = 400/3400, 550/850, 594/1120$) and (2) acetonitrile ($\lambda/\epsilon = 400/2100, 550/530, 594/690$). (B) Normalized fluorescence spectra of **2** ($\lambda_{\text{exc}} = 400 \text{ nm}$) in (1) methylcyclohexane, (2) benzene, (3) benzonitrile, and (4) acetonitrile.

explained by the fact that emission comes mostly from the CT state. Molecules with flexible geometry in the excited state exhibit low values of ϕ_{fl} because the energy is dissipated into rotational and vibrational activity.³¹ Thus, excitation of **2** in polar solvents produces a CT state with flexible geometry, as opposed to the rigid geometry of the ground state. A number of molecules, used as fluorescence probes, exhibit a dramatic increase in ϕ_{fl} with an increase of the viscosity–rigidity of the surrounding medium. Loutfy³² reported a class of compounds that display a 100-fold difference between the values of ϕ_{fl} in solution and in a rigid polymer such as poly(methyl methacrylate). He named them “molecular rotors” (Scheme 4).

To test whether **2** exhibits similar behavior, fluorescence spectra were compared in solution at -78°C and in organic

SCHEME 4: Examples of “Molecular Rotor” Fluorescence Probes

glass at -78°C . A quartz test tube containing a solution of **2** in either mineral oil or methylcyclohexane was cooled to -78°C in a spectroscopic Dewar equipped with a thermocouple. Mineral oil forms a stable glass in the -78 to -90°C temperature range, while methylcyclohexane is a viscous liquid at this temperature. Both are nonpolar solvents. The sample compartment of the fluorometer was purged with nitrogen to eliminate moisture, and the fluorescence spectra were recorded at -78°C . The solutions were then allowed to warm to room temperature in the fluorometer sample compartment. Then the room-temperature fluorescence spectra were recorded at $+23^\circ\text{C}$ (Figure 6A). The fluorescence maximum of **2** is at 615 nm in methylcyclohexane and 613 nm in mineral oil, and the shape of the emission spectrum is a mirror image of the absorption spectrum. An increase in the emission intensity at lower temperature is common. An increase in ϕ_{fl} of 1.3 times was observed in methylcyclohexane, which is a mobile liquid at both $+23$ and -78°C . However, the 5.6-fold increase in ϕ_{fl} of **2** in mineral oil at lower temperature is partially due to a more rigid environment, which implies that the geometry of the D₁ state of **2** is somewhat flexible.

The fluorescence spectra of **2** in polar 2-cyanoethyl acetate at different temperatures are shown in Figure 6B. Although at -78°C 2-cyanoethyl acetate is a viscous oil, a 12-fold increase in ϕ_{fl} was observed at lower temperature. This indicates a greater sensitivity of ϕ_{fl} in polar solvents toward the viscosity of the surrounding media. Therefore, the “molecular rotor” model can be applied toward the emitting state of **2** in polar solvents.

An organic glass of **2** in methylcyclohexane at 77 K was examined for phosphorescence emission. Since no phosphorescence was detected, there is no evidence that the quartet state of **2** is populated.

The electrochemistry of **2** was examined in acetonitrile in the presence of 0.1 M tetrabutylammonium perchlorate as the supporting electrolyte. Oxidation and reduction curves were

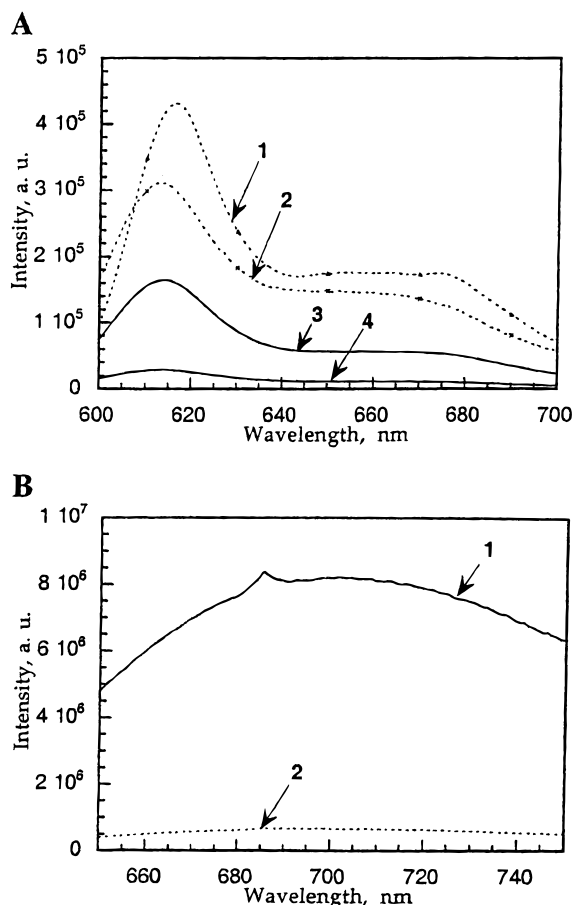


Figure 6. (A) Fluorescence of **2** in (1) methylcyclohexane, -78 °C; (2) methylcyclohexane, $+23$ °C; (3) mineral oil glass, -78 °C; (4) mineral oil liquid, $+23$ °C. (B) Fluorescence of **2** in 2-cyanoethyl acetate: (1) at -78 °C; (2) at $+23$ °C ($\lambda_{\text{exc}} = 590$ nm).

measured vs Ag/0.01 M AgNO₃ reference electrode. A value of $+0.21$ V vs SCE for the oxidation potential of **2** was calculated from the oxidation curve. This is comparable with the oxidation potential for 4,4',4''-trimethyltriphenylmethyl ($+0.29$ V vs SCE in 1,2-dimethoxyethane).³³ The reduction potential of **2** in acetonitrile (-0.87 V vs SCE) is comparable with that of 4,4',4''-trichlorotriphenylmethyl (-0.87 V vs Ag/AgCl in DMSO).³⁴ The oxidation and reduction potentials for **2** in acetonitrile vs SCE were calculated using the oxidation potential of ferrocene $E_{\text{ox}} = 0.063$ V in acetonitrile vs Ag, AgNO₃ and $E(\text{Ag}/0.01 \text{ M AgNO}_3/\text{TEAP}) = 0.291$ V vs SCE as a reference.³⁵

The Rehm–Weller equation gives a free energy value for an electron-transfer reaction between the first excited doublet state of radical R(D₁) and the ground doublet state R(D₀), which produces solvated ions.



$$\Delta G = E_{\text{ox}} - E_{\text{red}} - E_{00} + 2.6/\epsilon - 0.13$$

The excited-state energy E_{00} of **2** in benzene is 1.96 eV ($\lambda_{\text{max}}^{\text{fl}} = 633$ nm), in benzonitrile $E_{00} = 1.77$ eV ($\lambda_{\text{max}}^{\text{fl}} = 700$ nm), and in acetonitrile $E_{00} = 1.74$ eV ($\lambda_{\text{max}}^{\text{fl}} = 712$ nm). Therefore, the free energy of the electron-transfer reaction in benzene ΔG^{PhH} is $+0.14$ V, in benzonitrile $\Delta G^{\text{PhCN}} = -0.73$ V, and in acetonitrile $\Delta G^{\text{MeCN}} = -0.72$ V. Thus, the electron-transfer reaction is endothermic in benzene and exothermic in benzo-

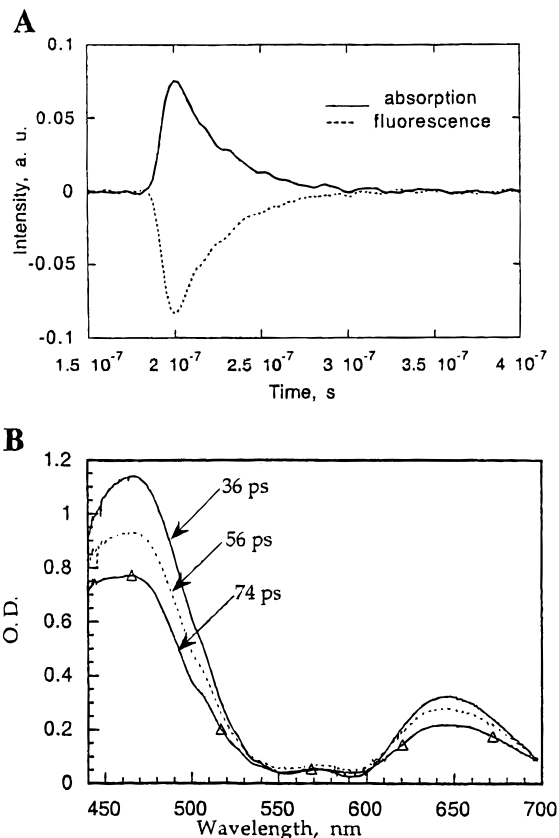


Figure 7. (A) Transient decay of D₁ state of **2** in benzene: absorption (467 nm), lifetime 26 ± 2 ns; fluorescence (680 nm), lifetime 25 ± 2 ns ($[\mathbf{2}] = 1.3 \times 10^{-3}$ M). (B) Transient absorption spectra of the D₁ state of **2** in acetonitrile (6.4×10^{-3} M).

trile and acetonitrile. For this reaction to be possible at $[\mathbf{2}] = 0.01$ M, the lifetime of D₁ should be at least a few hundred nanoseconds. However, transient absorption and fluorescence studies described next yielded the much shorter values of the D₁ lifetime.

(b) Laser Flash Photolysis. A solution of **2** in benzene (1.3×10^{-3} M) was investigated with nanosecond LFP. Decay of the fluorescence signal at 680 nm had a lifetime of 26 ± 2 ns, while the lifetime of the transient absorption centered at 467 nm was 25 ± 2 ns (Figure 7A). Therefore, the observed transient absorption in the 400–500 nm range is that of the D₁ state of **2** and corresponds to D₁ → D₂ transition.

Fluorescence lifetime measurements were performed for **2** in acetonitrile (2.3×10^{-3} M) and benzonitrile (3×10^{-3} M). Because of the low ϕ_{fl} of **2** in acetonitrile and the 8 ns resolution of the instrument, the lifetime of fluorescence at 712 nm was estimated to be on the order of 1–2 ns in acetonitrile. The fact that the observed fluorescence was that of **2** was confirmed when the fluorescence spectrum in acetonitrile was recorded 10 ns after the laser pulse. It was identical to that measured under the steady-state conditions. Experiments in benzonitrile yielded a value of 11 ± 2 ns for the observed fluorescence lifetime of **2**. No transient absorbance in the 400–500 nm region was detected in acetonitrile and benzonitrile on the nanosecond time scale. This suggests that an emitting state of **2** other than D₁ is populated in polar solvents.

Absorption of the D₁ state was detected in acetonitrile, when 532 nm laser pulses with 30 ps width were employed for the excitation ($[\mathbf{2}] = 6.4 \times 10^{-3}$ M, Figure 7B). A satisfactory fit of the transient absorption decay at 467 nm was obtained using first-order kinetics. The lifetime of the D₁ state of **2** in

TABLE 1: Photophysical Properties of 2 in Various Solvents^a

solvent	ϵ^b	η^b	λ_{\max}	λ_{fl}	ϕ_{fl}	$\tau(D_1)$	τ_{fl}	$10^4\phi_r$
PhH	2.27	0.649	596	633	0.44	25 ± 2	26 ± 2	9.0
PhCN	25.7	1.24	593	700	0.024	1.60 ± 0.07	11 ± 2	3.9
MeCN	37.5	0.345	592	712	0.001	0.126 ± 0.005	1–2	1.0

^a λ_{\max} is the absorption maximum, nm; λ_{fl} is the fluorescence emission maximum, nm; ϕ_{fl} is the quantum yield of fluorescence; $\tau(D_1)$ is the lifetime of the D_1 state, ns; τ_{fl} is the lifetime of the observed fluorescence, ns; ϕ_r is the quantum yield of the photoreaction. ^b From Murov, S. L.; Carmichael, I.; Hug, G. L. *Handbook of Photochemistry*; 1993. ϵ is the dielectric constant, and η is viscosity, cP.

acetonitrile was 126 ± 5 ps. The 640 nm peak at in Figure 7B belongs to D_1 as well, since the same decay parameters were obtained at this wavelength. In benzonitrile, the lifetime of D_1 was determined as 1.60 ± 0.07 ns.

Since the lifetimes of the D_1 state of the radical are in the 0.1–25 ns range, bimolecular reactions of D_1 with any other species but solvent molecules are of little significance.

(c) Summary. Photophysical parameters measured for **2** in various solvents are compiled in Table 1. Different values for the lifetime of the observed fluorescence and the lifetime of the first excited doublet state of **2** in polar solvents indicate the existence of two excited states: D_1 and CT. In nonpolar solvents such as benzene, excitation of the radical produces D_1 , which then decays via fluorescence and internal conversion. The absorption of D_1 ($D_1 \rightarrow D_2$) is observed, the lifetime of which equals the observed lifetime of fluorescence. The CT state is not populated in benzene because it is of higher energy than the D_1 state. In polar solvents such as acetonitrile, transition between the D_1 state of **2** and the CT state occurs, since the latter is lower in energy. The CT state of **2** has a flexible geometry. A tendency in ϕ_{fl} and ϕ_r (next section) shows that fluorescence and the photoreaction are more efficient for the D_1 state, while efficient internal conversion is the primary decay pathway for the CT state.

(d) Photoreaction of 2 in Various Solvents. Upon exposure of a solution of **2** to visible or UV light, a slow bleaching process is observed. The rate of bleaching varies in different solvents. Quantum yields of reaction (ϕ_r) were determined in benzene, benzonitrile, and acetonitrile. When determining ϕ_r , it is necessary to account for the change in the absorption of the radical. Equation 5 for ϕ_r is derived in the Experimental Section. To determine the quantum yield of radical disappearance, solutions of **2** were irradiated with a 514 nm line of an Ar-ion laser and the absorption of **2** was measured at certain times (Figure 8A). A plot of $-\log((1-T)/T)$ vs time is shown in Figure 8B for **2** in benzonitrile. Substitution of values of ϵ of **2** at 514 nm, I_0 (light intensity, 3.5×10^{-7} einstein/s), and path length into eq 5 gave the values of ϕ_r : 9×10^{-4} , 3.9×10^{-4} , and 1.0×10^{-4} in benzene, benzonitrile, and acetonitrile, respectively. Therefore, the efficiency of the photoreaction is generally low and is lower in more polar solvents.

Benzene was chosen as a solvent for two separate preparative photolyses.^{23,24} In the first, a 100 mL solution (5×10^{-3} M) was irradiated for 12 h with light from a 300 W tungsten lamp, which was filtered through a NaNO_2 solution (400–800 nm). The photolysis was stopped when the red color of **2** disappeared. The residue obtained after evaporation of the solvent was treated with ethyl acetate, and an insoluble white precipitate was filtered. It was identified as tetrakis(4-*tert*-butylphenyl)ethylene (**21**) (yield 20%). GC/MS analysis of the photolyzate showed no benzophenone. The photolyzate was not analyzed further.

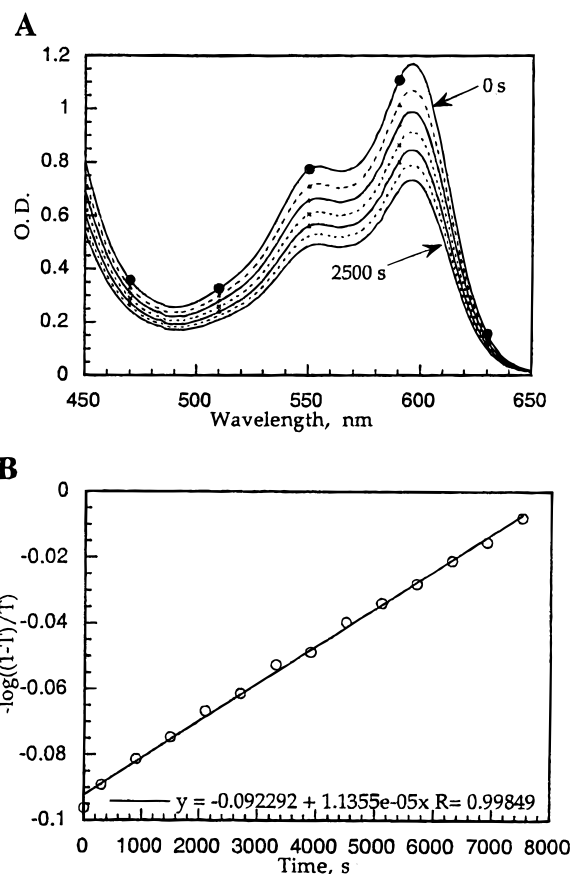


Figure 8. (A) Photolysis of **2** in benzene (0 s \rightarrow 2500 s at 360 s increments). (B) Photolysis of **2** (2.3×10^{-3} M) in benzonitrile.

In the second run, a 300 mL benzene solution was irradiated with a 500 W tungsten halogen lamp (350–800 nm) and water was used as a filtering–cooling solution. Upon exposure of a 0.012 M solution of **2** (1.7 g) in degassed benzene to visible light for 31 h, the red color of the radical slowly disappeared. The yellow solution of the photolyzate was exposed to air and analyzed. The best separation of the roughly 20 spots of which four were major (TLC) was achieved with ethyl acetate/hexanes = 1/15. Eluting ethyl acetate/hexanes = 1/33 over a silica column provided the best separation by HPLC and showed a total of 22 peaks of which 9 were major. After evaporation of solvent, the photolyzate was subjected to preparative TLC followed by Soxhlet extraction. (*p*-Benzoylphenyl)bis(4-*tert*-butylphenyl)methanol (**18**) was recovered, and the conversion of **2** was presumed to be 91%. The photoproducts are listed in Table 2. Products **16**, **18**, **20**, and **21** were isolated, purified, and identified. Compounds **18** and **21** were found identical to the known materials. The rest of the photoproducts were separated in mixtures of two to three compounds and not purified but characterized primarily by GS/MS and TLC. An inseparable mixture of the unidentified low-yield products constituted about 20% of the photolyzate.

A trapping experiment was attempted. Degassed toluene was added to a benzene solution of **2**. This resulted in a ground-state reaction since in 2 h the color of radical **2** disappeared in the dark.

Isolation of a dominant H-abstraction product, triarylmethane **20**, came as a surprise because we assumed absence of H-donors such as the dimer of **2** in the system. This assumption might have been incorrect. The color of **2** could disappear during the preparative photolysis partially due to dimerization (ground state and/or photoinduced). Upon exposure to air, the dimer of **2** could

TABLE 2: Products from Irradiation of 2 in Degassed Benzene, Molar %

#	structure	yield
18		9
19		1
20		56
21		5
22		10
23		6
16		6
24		4
25		4
26		2
27		2
28		2
29		0.5

produce carbinol **18** (yield 9%) as well as other products of oxidation. Alternative H-donors could be intermediates derived from cyclization reactions of **2** that lead to the formation of fluorene derivatives **23**, **26**, **28**, and **29**. Formation of ethylene **21** suggests the intermediacy of bis(4-*tert*-butylphenyl)carbene and *p*-benzoylphenyl, although neither the dimer of *p*-benzoylphenyl nor benzophenone was detected. Instead, 4-hydroxybenzophenone (**22**) was isolated in 2:1 molar ratio to **21**.

Interestingly, phenanthrene **27**, which is the photocyclization product of ethylene **21**, was detected.

The apparent extinction coefficients of **2** in benzene and acetonitrile (Figure 5A) were calculated assuming that no dimerization of **2** occurred. Their values are significantly lower than ϵ of **1** in acetonitrile that we have derived above. This indicates that the dimerization of **2** might have persisted. One possible reason is that the *p*-benzoyl group is not bulky enough.

Though it was unexpected, the photoproducts of **2** in benzene differ slightly from those of **1**. Products of H-abstraction account for 50–60% of the converted radical, while products of fragmentation account for ~20%, and cyclization products account for only ~10%. Although our mechanistic study is far from complete, we propose formation of diarylcarbene and *p*-benzoylphenyl takes place. The products of this fragmentation in benzene should be formed via initial C–C bond cleavage in the excited radical. On the basis of the average value for a C–C bond dissociation energy (85 kcal/mol) and the energy of the excited radical (45 kcal/mol in benzene), as well as the low value of the quantum yield of fragmentation (2×10^{-4}), we conclude that this reaction may require absorption of at least two visible-light photons. To confirm this, the dependence of the reaction rate on the intensity of the absorbed light must be studied.

Conclusions

Investigation of the photophysics of **1** and **2** resulted in development of a molecular model characterizing their behavior: both radicals follow the “molecular rotor” model in their excited-state chemistry.

The photochemistry of these stable radicals is complicated by the propensity to dimerize. The difference in the photoproducts of **1** and **2** is minor. We postulate that the photochemistry of **1** is dominated by H-abstraction due to reaction of **1*** with dimer **5**. But in **2**, where dimer formation was thought to have been eliminated, similar products were obtained. The H-abstraction reaction (50–60%) dominates in the case of **2** as well. Other reactions occur: fragmentation (10–20%), cyclization (5–15%), and possibly addition (photoinduced dimerization of two radicals, 10–20%). To occur to an appreciable extent, the rate constant of the addition reaction should be at least 10^7 – 10^8 M⁻¹ s⁻¹.

Experimental Section

Materials and Equipment. Reagents and solvents were purchased from Aldrich. Benzene (99%+, thiophene-free) and THF (anhydrous, 99.8%) were distilled under argon from Na–benzophenone prior to use. Acetonitrile (99.9%+, HPLC grade) was distilled from P₂O₅ under argon, and benzonitrile (99%+, anhydrous) was purged with argon at 75 °C. Solvents used without purification were spectrophotometric grade. NMR spectra were taken with either a Varian Gemini 200 NMR or a Varian Unity Plus 400 NMR spectrometer. Chemical shifts are in ppm with either TMS or residual nondeuterated solvent as the internal standard. GC/MS and DIP/MS were taken on an HP 5988 mass spectrometer coupled to an HP 5880A GC with a 30 m × 0.25 mm i.d. × 0.25 mm film thickness DB-5 ms column, interfaced to an HP 2623A data processor. UV–visible spectra were obtained using an HP 8452 diode array spectrophotometer. Infrared spectrometry was performed using a Mattson Instruments 6020 Galaxy Series FT-IR spectrometer. Elemental analysis was carried out by Atlantic Microlab Inc. HRMS was performed at the University of Illinois Urbana-Champaign, School of Chemical Sciences. Melting points were

determined using a capillary melting point apparatus (Uni-melt, Arthur H. Thomas Co., Philadelphia) and were uncorrected. HPLC analysis was performed on a HP 1050 series instrument using a multiple wavelength diode array detector. Separations at a flow rate of 1 mL/min were performed on either a Nucleosil AB (Altech) 15×4.6 mm column, using $\text{H}_2\text{O}/\text{MeCN} = 1/5$ as eluent or Hypersil (HP) 20×4.6 mm column with hexane/EtOAc = 15/1.

Fluorescence Measurements. Fluorescence spectra were recorded with a SPEX Fluorolog 2 spectrofluorometer equipped with both excitation and emission double beam monochromators. Spectra were measured in perpendicular geometry using a 1 cm quartz cuvette. All spectra were corrected (band-pass 2.8 nm). Fluorescence quantum yields of radicals in solution were measured using cresyl violet acetate in ethanol ($\phi_{\text{fl}} = 0.50 \pm 0.02$)³⁶ as a reference solution. The values of ϕ_{fl} were calculated as: $\phi_{\text{fl}} = \phi_{\text{ref}} I_{\text{fl}}(1 - T_{\text{ref}})/(I_{\text{ref}}(1 - T))$, where ϕ_{ref} is a quantum yield of fluorescence of the reference, I_{fl} and I_{ref} are fluorescence intensities of the unknown and the reference, and T and T_{ref} are the transmittances of the unknown and the reference at the wavelength of excitation.

Quantum Yield of Radical Disappearance. A solution of the radical in a cuvette was irradiated with 514 nm line of an air-cooled Ar-ion laser (OmNichrome, model 543). This line was isolated with an interference filter (Oriel, 6 nm band-pass). Laser power was measured with a power meter (Scientech 365). Absorbance of the radical in solution at 514 nm was measured at certain times during irradiation.

The following factors were considered in the calculation of ϕ_r . Let us consider a photochemical reaction of a compound R excited by monochromatic light: $\text{R} + h\nu \rightarrow \text{R}^* \rightarrow \text{products}$. The rate of disappearance of R is proportional to the number of photons absorbed by R in a unit of time: $-dc/dt = \phi_r I_a$ (1), where c is concentration of R in M, t is time in seconds, ϕ_r is quantum yield for the photochemical reaction of R, and I_a is photon flux absorbed by R in einsteins/s. From Beer's law: $c = A/l\epsilon$ (2), where A is the absorbance of R at a given wavelength, ϵ is an extinction coefficient of R at this wavelength in $\text{M}^{-1} \text{cm}^{-1}$, and l is a path length in cm. Thus, $-dA/dt = l\epsilon\phi_r I_a$ (3). I_a can be expressed as $I_a = I_0(1 - T)$, where I_0 is a total photon flux and T is transmittance of solution of R at the wavelength of excitation. $T = 10^{-A}$ and $A = -\log T$. Substituting these expressions into eq 3 results in: $d(\log T)/dt = l\epsilon\phi_r I_0(1 - T)$ (4). Integrating yields: $\log(T/(1 - T)) = 2.3l\epsilon\phi_r I_0 t$ (5).

Electrochemical Characterization. A solution of radical 2 (1×10^{-3} M) and tetrabutylammonium perchlorate (0.1 M) in acetonitrile was placed in a 15 mL electrochemical cell equipped with a working platinum electrode, an auxiliary electrode (platinum wire), and a reference electrode (Ag, 0.01 M AgNO_3 //0.1 M TBAP in MeCN). The solution was kept under argon during the measurements, which were performed on a BAS 100A Electroanalytical analyzer with a scan rate of 200 mV/s. At the end of the experiment a small amount of ferrocene (99.8%) was added to the cell, and the oxidation potential was determined. This value was used to correct the values of redox potentials measured for 2.

Laser Flash Photolysis. Nanosecond pulsed laser photolyses were carried out on a setup described by Ford and Rodgers using the second harmonic of a Q-switched Nd:YAG laser (Continuum, YG660) as a pump light (fwhm 8 ns).³⁷ The instrument was used in both absorption and emission modes. Picosecond LFP experiments were performed on a setup described by Logunov and Rodgers.³⁸ Laser pulses of 30 ps width were

generated by the second harmonic (532 nm) of Nd:YAG laser (Quantel YG571C). The 50 mL sample solution was placed in an optical glass cuvette connected with a 100 mL Schlenk tube. The large volume of the sample solution allowed minimization of the effect of radical bleaching during the measurements. The solution in the cuvette was stirred continuously during the experiment.

Steady-State Photolysis. Photolyses were performed under a dry argon atmosphere. For UV-light irradiation, a benzene solution of the radical in a 250 mL Pyrex test tube was placed in a Rayonet RPR-100 photoreactor (a merry-go-round apparatus) equipped with 14 350 nm filter-coated GE F8T5 (24 W) low-pressure mercury UV bulbs ($\lambda_{\text{exc}} \sim 330\text{--}370$ nm), a stirring plate, and a cooling fan. For visible-light photolysis a tungsten halogen lamp was used ($\lambda_{\text{exc}} = 350\text{--}800$ nm).

Preparative Photolysis of 2 (#1). Irradiation was performed in an Ace Glass photochemical reactor (100 mL) using a 300 W tungsten lamp. The reactor was cooled internally by circulating a solution of NaNO_2 (75 g/L) in H_2O to cut off UV light (<400 nm) generated by the lamp. Irradiation was continued until complete disappearance of the radical was assured. The residue obtained after evaporation of benzene was dissolved in 20 mL of ethyl acetate, and the insoluble white solid was filtered.

Preparative Photolysis of 2 (#2). Radical 2 (1.7 g, 3.7 mmol) was prepared via addition of Cu powder (17:1) to chloride 19 (1.92 g, 3.9 mmol). The synthesis, handling, and photolysis were done under argon. Preparative photolysis of 0.012 M solution in benzene (300 mL) was performed in an Ace Glass photochemical reactor (500 mL) using a 500 W tungsten halogen lamp. The reactor was cooled internally by circulating water. Irradiation was continued until the red color of the radical disappeared. After irradiation the solution was exposed to air, and oxidation occurred. The residue obtained after evaporation of benzene was dissolved in 10 mL of dichloromethane. The unreacted starting material and products were separated on 20×20 cm silica gel plates ($2000 \mu\text{m}$, $5\text{--}17 \mu\text{m}$, 60 \AA , Altech) with hexane/ethyl acetate = 15/1, purified, weighed, and identified. Compounds were characterized by ^1H and ^{13}C NMR, mass, IR, and UV-vis spectroscopy, elemental analysis, HRMS, HPLC, and TLC. For low-yield and inseparable compounds, TLC and GC-DIP/MS results are reported.

Photoproducts. (*p*-Benzoylphenyl)bis(4-*tert*-butylphenyl)methane (20): ^1H NMR (200 MHz, CDCl_3) δ 7.81–7.66 (m (d, dd), 4H), 7.59–7.47 (m, 1H), 7.47–7.36 (d, 2H), 7.35–7.27 (d, $J = 8.4$ Hz, 4H), 7.27–7.18 (d, $J = 8.4$ Hz, 2H), 7.10–6.98 (d, $J = 8.4$ Hz, 4H), 5.54 (s, 1H(CH)), 1.29 (s, 18H); ^{13}C NMR (APT, 50 MHz, CDCl_3) δ 196.3, 149.4, 149.2, 140.1, 137.7, 135.4, 132.1, 130.1, 129.9, 129.3, 128.9, 128.1, 125.2, 56.0, 34.3, 31.3; MS (EI) 460, 445, 403, 355, 278, 215, 176, 162, 117, 105 (b), 77, 57. Anal. Calcd for $\text{C}_{34}\text{H}_{36}\text{O}$: C, 88.65; H, 7.87. Found: C, 88.71; H, 7.82.

Tetrakis(4-*tert*-butylphenyl)ethylene (21):³⁹ ^1H NMR (200 MHz, CDCl_3) δ 7.33–7.25 (d, $J = 8.4$ Hz, 8H), 7.13–7.03 (d, $J = 8.4$ Hz, 8H), 1.24 (s, 36H); C_6D_6 δ 7.10–7.02 (d, $J = 8.4$ Hz, 4H), 6.96–6.87 (d, $J = 8.4$ Hz, 4H), 1.14 (s, 36H); ^{13}C NMR (APT, 50 MHz, CDCl_3) δ 148.8, 141.1, 140.2, 130.9, 124.1, 34.3, 31.3; C_6D_6 δ 149.1, 142.0, 140.7, 131.7, 124.9, 34.4, 31.3; MS (EI) 556, 541, 263, 57 (b), 41; mp 342 °C, dec; UV-vis 312 nm.

Other: MS (EI): (22) 198, 121 (b), 105, 93, 77, 51, 39; (23) 474, 417, 402, 361, 222, 161, 105 (b), 77, 57; (25) 342, 327 (b), 271, 209, 161, 152, 105, 77; (26) 292, 277 (b), 249,

178, 131, 117, 103, 57; (27) 554, 539, 262, 57; (28) 458, 402, 353, 214, 105 (b), 77, 57.

Synthesis of 1. (*p*-Benzoylphenyl)diphenylmethanol (**3**) was synthesized from 4-(trifluoromethyl)benzophenone via Friedel–Crafts reaction in benzene using a procedure described by Neckers et al.⁴⁰ and purified by recrystallization from methanol (91% yield, mp 131 °C).²² (*p*-Benzoylphenyl)diphenylmethyl chloride (**4**) was prepared from carbinol **3** via reaction with thionyl chloride in refluxing benzene for 4 h. Chloride **4** was purified by repeated recrystallization from glacial AcOH/AcCl (5/1 by volume) according to Wittig et al. (yield 64%, mp 122 °C).²² Radical **1** was prepared from **4** by Gomberg's method² with Ag powder (2.5 μm).

Synthesis of 2. The Friedel–Crafts reaction of 4-(trifluoromethyl)benzophenone with 2 equiv of *tert*-butylbenzene in the presence of 2 equiv of AlCl₃ led to many byproducts due to migration of *tert*-butyl group.⁴¹ However, reaction of the Grignard reagent formed from acetal **14** with benzophenone **16** was successful.

4-Bromobenzophenone Acetal (14).⁴² Solution of 4-bromobenzophenone (11 g, 42.1 mmol), ethylene glycol (20 mL, 354 mmol), and a catalytic amount of *p*-toluenesulfonic acid (500 mg) in 150 mL of toluene was refluxed for 10 h. Water was removed from the reaction mixture by azeotropic distillation. The reaction mixture was washed with 10% Na₂CO₃ and aqueous NaCl and dried over MgSO₄. The solvent was evaporated, and the product was recrystallized from ethanol (yield 86%, mp 56 °C).

4,4'-Di-*tert*-butylbenzophenone (16).⁴³ 4-*tert*-Butylbenzoyl chloride (10 g, 51 mmol), *tert*-butylbenzene (8 g, 60 mmol), and AlCl₃ (7.3 g, 55 mmol) were dissolved in 30 mL of dry nitrobenzene. The solution was stirred at 25 °C for 20 h and then at 60 °C for 2 h. Nitrobenzene was removed by steam distillation, and the resulting solid was recrystallized twice from ethanol (yield 79%, mp 131–132 °C). ¹H NMR (200 MHz, CDCl₃) δ 7.81–7.71 (d, *J* = 8.8 Hz, 4H), 7.53–7.44 (d, *J* = 8.8 Hz, 4H), 1.37 (s, 18H); ¹³C NMR (APT, 50 MHz, CDCl₃) δ 155.9, 135.1, 130.0, 125.1, 35.1, 31.1; MS (EI) 294, 279(b), 237, 161, 146, 132, 118, 104, 91, 77, 57, 41.

(*p*-Benzoylphenyl)bis(4-*tert*-butylphenyl)methanol (18). Solution of acetal **14** (3.05 g, 10 mmol) in THF (20 mL) was added dropwise over 30 min to a stirred suspension of activated magnesium in THF (20 mL), which was prepared by the procedure of Rieke and Bales⁴⁴ from anhydrous MgCl₂ (1.92 g, 20 mmol), KI (1.68 g, 10 mmol) and K (1.39 g, 35.8 mmol). The mixture was further stirred for 2 h, and a solution of **16** (2.94 g, 10 mmol) in 20 mL of THF was added. The reaction mixture was stirred at 50 °C for 24 h. After treatment with saturated NH₄Cl at 0 °C, the mixture was extracted with ether. After removal of the solvent, a yellow oil was obtained, to which 50 mL of water, 100 mL of THF, and 0.8 g of TsOH were added. The mixture was refluxed for 8 h. After evaporation of THF, 200 mL of ether was added, and the solution was extracted with 10% Na₂CO₃, water, and aqueous NaCl. The solvent was evaporated, and the crude product was chromatographed on silica gel with hexane/ethyl acetate (20/1). The separated carbinol was recrystallized from petroleum ether (yield 49%). Mp: 151–152 °C. ¹H NMR (200 MHz, CDCl₃): δ 7.8–7.66 (m (d, dd), 4H), 7.59–7.48 (m, 1H), 7.48–7.35 (m (d, d), 4H), 7.35–7.24 (d, *J* = 8.6 Hz, 4H), 7.23–7.12 (d, *J* = 8.6 Hz, 4H), 3.12 (s, 1H(OH)), 1.3 (s, 18H). ¹³C NMR (APT, 50 MHz, CDCl₃): δ 196.4, 151.6, 150.2, 143.4, 137.5, 135.9, 132.3, 130.0, 129.6, 128.2, 127.7, 127.5, 124.9, 81.5, 34.4, 31.3. IR (KBr), cm⁻¹: 3490, 2962, 2902, 2866, 1656, 1605, 1446, 1319,

1314, 1283, 730, 600. MS (EI): 476, 459–61, 403, 343, 315, 295 (b), 209, 161, 105 (b), 77, 57, 41. HRMS Calcd for C₃₄H₃₆O₂: 476.2710. Found: 476.2715. Purity: 99%, HPLC.

(*p*-Benzoylphenyl)bis(4-*tert*-butylphenyl)methyl Chloride (19). Carbinol **18** (1 g, 2.1 mmol) in anhydrous benzene (20 mL) was heated to reflux. Thionyl chloride (99.9%+, 3 mL) in 5 mL of anhydrous benzene was added through the reflux condenser. The mixture was refluxed for 4 h. The solvent was evaporated, and the crude product recrystallized from anhydrous petroleum ether (yield 95%). Mp: 212–213 °C (dec). IR (KBr), cm⁻¹: 2965, 2904, 2868, 1655, 1599, 1506, 1477, 1462, 1449, 1401, 1317, 1310, 1276, 703, 610. MS (EI): 459, 402, 326. Anal. Calcd for C₃₄H₃₅OCl: C, 82.52; H, 7.08. Found: C, 82.68; H, 7.13.

Radical **2** was produced from **19** by reaction with either Cu powder (99%, submicron) in benzene at 80 °C for 2 h or Ag powder (99.99%, 2.5 μm) at room temperature in acetonitrile.² Heating of the radical in acetonitrile resulted in its decomposition. The reaction was stopped after Beilstein test produced negative result. Sensitivity of the test is in the microgram region,²⁷ thus quantitative conversion of **19** was assumed. ¹H NMR (200 MHz, C₆D₆): δ 7.75–7.50 (m (d, d), 4H), 7.50–6.95 (m, 13H), 1.15 (s, 18H).

Synthesis of 2-Cyanoethyl Acetate. 3-Hydroxypropionitrile (20 g, 280 mmol) was reacted with acetic anhydride (300 g) in anhydrous pyridine (500 mL) for 24 h. Excess acetic anhydride, acetic acid, and pyridine were evaporated under reduced pressure. The remaining yellow oily liquid was distilled under 1 mmHg to give 28 g (89% yield) of 2-cyanoethyl acetate. ¹H NMR (CDCl₃): δ 2.11 (3H, s), 2.708 (2H, t, *J* = 6.34 Hz), 4.272 (2H, t, *J* = 6.34 Hz).

Acknowledgment. We thank Drs. George S. Hammond and Thomas H. Kinstle for insightful discussions. We are indebted to Dr. Michael A. J. Rodgers for use of his LFP facilities. Both V.J. and A.N. are grateful to the McMaster Endowment for a Fellowship.

References and Notes

- (1) Contribution No. 402 from the Center for Photochemical Sciences.
- (2) Gomberg, M. *J. Am. Chem. Soc.* **1900**, 22, 757.
- (3) Forrester, A. R.; Hay, J. M.; Thompson, R. H. *Organic Chemistry of Stable Free Radicals*; Academic Press: New York, 1968.
- (4) Johnston, L. J. *Chem. Rev.* **1993**, 93, 251.
- (5) Wilson, R. M.; Schnapp, K. A. *Chem. Rev.* **1993**, 93, 223.
- (6) Johnston, L. J.; Scaiano, J. C. *Chem. Rev.* **1989**, 89, 521.
- (7) Scaiano, J. C.; Johnston, L. J. *Org. Photochem.* **1989**, 10, 309.
- (8) Caldwell, R. In *Kinetics and Spectroscopy of Carbenes and Biradicals*; Platz, M. S., Ed.; Plenum Publishing Corp.: New York, 1990; p 77.
- (9) Smirnov, V. A.; Plotnikov, V. G. *Russ. Chem. Rev.* **1986**, 55, 929.
- (10) Duxbury, D. F. *Chem. Rev.* **1993**, 93, 381.
- (11) Letsinger, R. L.; Collat, R.; Magnusson, M. *J. Am. Chem. Soc.* **1954**, 76, 4185.
- (12) Siskos, M. G.; Zarkadis, A. K.; Steenken, S.; Karakostas, N.; Garas, S. K. *J. Org. Chem.* **1998**, 63, 3251 and references therein.
- (13) Fox, M. A.; Gaillard, E.; Chen, C. *J. Am. Chem. Soc.* **1987**, 109, 7088.
- (14) Faria, J. L.; Steenken, S. *J. Phys. Chem.* **1993**, 97, 1924.
- (15) Neckers, D. C.; Rajadurai, S.; Valdes-Aguilera, O.; Zakrzewski, A.; Linden, S. M. *Tetrahedron Lett.* **1988**, 29, 5109.
- (16) Scaiano, J. C.; Tanner, M.; Weir, D. *J. Am. Chem. Soc.* **1985**, 107, 4396.
- (17) Neumann, W. P.; Uzick, W.; Zarkadis, A. K. *J. Am. Chem. Soc.* **1986**, 108, 3762.
- (18) Neumann, W. P.; Penenory, A.; Stewen, U.; Lehnig, M. *J. Am. Chem. Soc.* **1989**, 111, 5845.
- (19) Bordwell, F. G.; Zhang, X.; Alnajjar, M. S. *J. Am. Chem. Soc.* **1992**, 114, 7623.
- (20) Lehnig, M.; Stewen, U. *Tetrahedron Lett.* **1989**, 30, 63.
- (21) Adrian, F. J. *J. Chem. Phys.* **1958**, 28, 608.

- (22) Wittig, G.; Kairies, W.; Hopf, W. *Chem. Ber.* **1932**, *65*, 767.
- (23) Nikolaitchik, A. V. Ph.D. Dissertation, Bowling Green State University, Bowling Green, OH, 1996.
- (24) Jarikov, V. V. Ph.D. Dissertation, Bowling Green State University, Bowling Green, OH, 1999.
- (25) Takeuchi, H.; Nagai, T.; Tokura, N. *Bull. Chem. Soc. Jpn.* **1971**, *44*, 753.
- (26) Zarkadis, A. K.; Neumann, W. P.; Uzick, W. *Chem. Ber.* **1985**, *118*, 1183.
- (27) Dittrich, H.; Vorberg, B. *Anal. Chim. Acta* **1982**, *140*, 237.
- (28) Nonhebel, D. C.; Walton, J. C. *Free-radical Chemistry*; University Press: Cambridge, 1974.
- (29) Kupchan, S. M.; Wormser, H. C. *J. Org. Chem.* **1965**, *30*, 3792.
- (30) Selwood, P. W.; Dobres, R. M. *J. Am. Chem. Soc.* **1950**, *72*, 3860.
- (31) Turro, N. J. *Modern Molecular Photochemistry*; University Science Books: Mill Valley, CA, 1991.
- (32) Loufty, R. O. *Pure Appl. Chem.* **1986**, *58*, 1239.
- (33) Bank, S.; Ehrlich, C. L.; Zubieta, J. A. *J. Org. Chem.* **1979**, *44*, 1454.
- (34) Breslow, R.; Chu, W. *J. Am. Chem. Soc.* **1973**, *95*, 411.
- (35) Mann, C. K.; Barnes, K. K. *Electrochemical Reactions in Non-aqueous Systems*; Dekker: New York, 1970.
- (36) Lopez-Arbeloa, I.; Rohatgi-Mukherjee, K. K. *Chem. Phys. Lett.* **1986**, *129*, 607.
- (37) Ford, W. E.; Rodgers, M. A. J. *J. Phys. Chem.* **1994**, *98*, 3822.
- (38) Logunov, S. L.; Rodgers, M. A. J. *J. Phys. Chem.* **1992**, *96*, 2915.
- (39) Smith, W. B. *Org. Magn. Reson.* **1981**, *15*, 317.
- (40) Neckers, D. C.; Linden, S.-M.; Williams, B. L.; Zakrzewski, A. J. *Org. Chem.* **1989**, *54*, 131.
- (41) Kulka, M. *J. Am. Chem. Soc.* **1954**, *76*, 5469.
- (42) Masuhara, H.; Maeda, Y.; Nakajo, H.; Mataga, K. N.; Tomita, K.; Tatemitsu, H.; Sakata, Y.; Misumi, S. *J. Am. Chem. Soc.* **1981**, *103*, 634.
- (43) Wagner, P. J.; Truman, R. J.; Puchalski, A. E.; Wake, R. *J. Am. Chem. Soc.* **1986**, *108*, 7727.
- (44) Rieke, R. D.; Bales, S. E. *J. Am. Chem. Soc.* **1974**, *96*, 1775.